

# miR-892b Inhibits Hypertrophy by Targeting KLF10 in the Chondrogenesis of Mesenchymal Stem Cells

Jong Min Lee,<sup>1,3</sup> Ji-Yun Ko,<sup>1,3</sup> Hye Young Kim,<sup>1</sup> Jeong-Won Park,<sup>1</sup> Farshid Guilak,<sup>2</sup> and Gun-Il Im<sup>1</sup>

<sup>1</sup>Research Institute for Integrative Regenerative Biomedical Engineering, Dongguk University, Goyang 10326, Republic of Korea; <sup>2</sup>Department of Orthopaedic Surgery, Washington University and Shriners Hospitals for Children–St. Louis, St. Louis, MO 63110, USA

**We investigated the functional role of miR-892b as a novel inhibitor of chondrocyte hypertrophy during TGF- $\beta$ -mediated chondrogenesis of human mesenchymal stem cells (hMSCs). The expression of miR-892b during TGF- $\beta$ -mediated chondrogenesis of hMSCs and the effects of miR-892b overexpression on chondrogenic and hypertrophic marker genes in the chondrogenesis of hMSCs were investigated. Targets of miR-892b were identified and verified by overexpression of synthetic miRNA mimics and luciferase assays. Cross-talk between Kruppel-like factor 10 (KLF10) and Indian hedgehog (Ihh) was investigated using KLF10 knockdown (KD). miR-892b enhanced chondrogenic makers and suppressed hypertrophy in hMSC chondrogenesis, mimicking parathyroid hormone-related peptide (PTHrP). KLF10, a transcription factor and miR-892b target, directly regulated Ihh promoter activity. Like miR-892b, KLF10 KD enhanced hMSC chondrogenesis and inhibited hypertrophy. Our findings suggest a key role of miR-892b in targeting the KLF10-Ihh axis as a regulator of hypertrophy in TGF- $\beta$ -mediated chondrogenesis of hMSCs and provide a novel strategy for preventing hypertrophy in chondrogenesis from MSCs.**

## INTRODUCTION

In transforming growth factor (TGF)- $\beta$ -mediated chondrogenesis of mesenchymal stem cells (MSCs), terminally differentiated chondrocytes spontaneously undergo hypertrophic maturation.<sup>1,2</sup> In contrast, hypertrophic signals are significantly reduced when MSCs undergo alternative TGF- $\beta$ -independent chondrogenic differentiation processes, such as transfecting the sex-determining region (SRY)-box transcription factor 5 (Sox5), -6, or -9 genes<sup>3–5</sup> or co-culturing MSCs and chondrocytes.<sup>6–8</sup> However, the utilization of MSCs in cartilage tissue engineering fields has been hampered by the lack of understanding of the causal connections between TGF- $\beta$  and the parathyroid hormone-related peptide (PTHrP)-Indian hedgehog protein (Ihh) feedback-regulatory loop during chondrogenic MSC maturation.

MicroRNAs (miRNAs) are small, single-stranded, noncoding RNAs found in diverse organisms that negatively regulate target-gene expression by either mRNA degradation or translational inhibi-

tion.<sup>9,10</sup> miRNAs can affect target-gene expression during MSC chondrogenesis in several species.<sup>11–13</sup> However, the precise roles of miRNAs in chondrocyte hypertrophy remain unknown, and the individual target genes of miRNAs in the process remain to be identified.

Our previous study suggested that PTHrP treatment during TGF- $\beta$ -mediated MSC chondrogenesis can markedly down-modulate hypertrophic markers in differentiated chondrocytes.<sup>5,14</sup> Here, we focused on miR-892b, which was induced by additional PTHrP treatment during TGF- $\beta$ -mediated MSC chondrogenesis. Lentivirus-mediated miR-892b overexpression enhanced the chondrogenic potential of MSCs and markedly reduced the expression of hypertrophic markers. Interestingly, Kruppel-like factor 10 (KLF10; also known as TGF- $\beta$ -inducible early growth-response protein 1 [TIEG1]) was shown to be a target of miR-892b and also to act as a transcription factor that directly regulated Ihh expression by binding the 5'-<sup>710</sup>GGCGGGG<sup>-703</sup>-3' element of the Ihh promoter. Here, we examine the hypothesis that miR-892b plays an essential role in the known PTHrP-Ihh feedback-regulatory loop by inhibiting KLF10. Our results reveal a new PTHrP-Ihh feedback-regulatory mechanism in MSC chondrogenesis and a strong rationale for developing miR-892b as a therapeutic agent to inhibit hypertrophy and enhance MSC chondrogenesis in cartilage tissue engineering.

## RESULTS

### miR-892b Induction by PTHrP in a Chondrogenic Culture of Human MSCs (hMSCs)

A commercial microarray was used to identify candidate miRNAs regulated by PTHrP treatment in chondrogenic hMSC differentiation. miRNA expression patterns from the 3-week-cultured pellets

Received 8 November 2018; accepted 31 May 2019;  
<https://doi.org/10.1016/j.omtn.2019.05.029>.

<sup>3</sup>These authors contributed equally to this work.

**Correspondence:** Gun-Il Im, MD, PhD, Research Institute for Integrative Regenerative Biomedical Engineering, Dongguk University, Goyang 10326, Republic of Korea.

**E-mail:** [imgunil@hanmail.net](mailto:imgunil@hanmail.net)



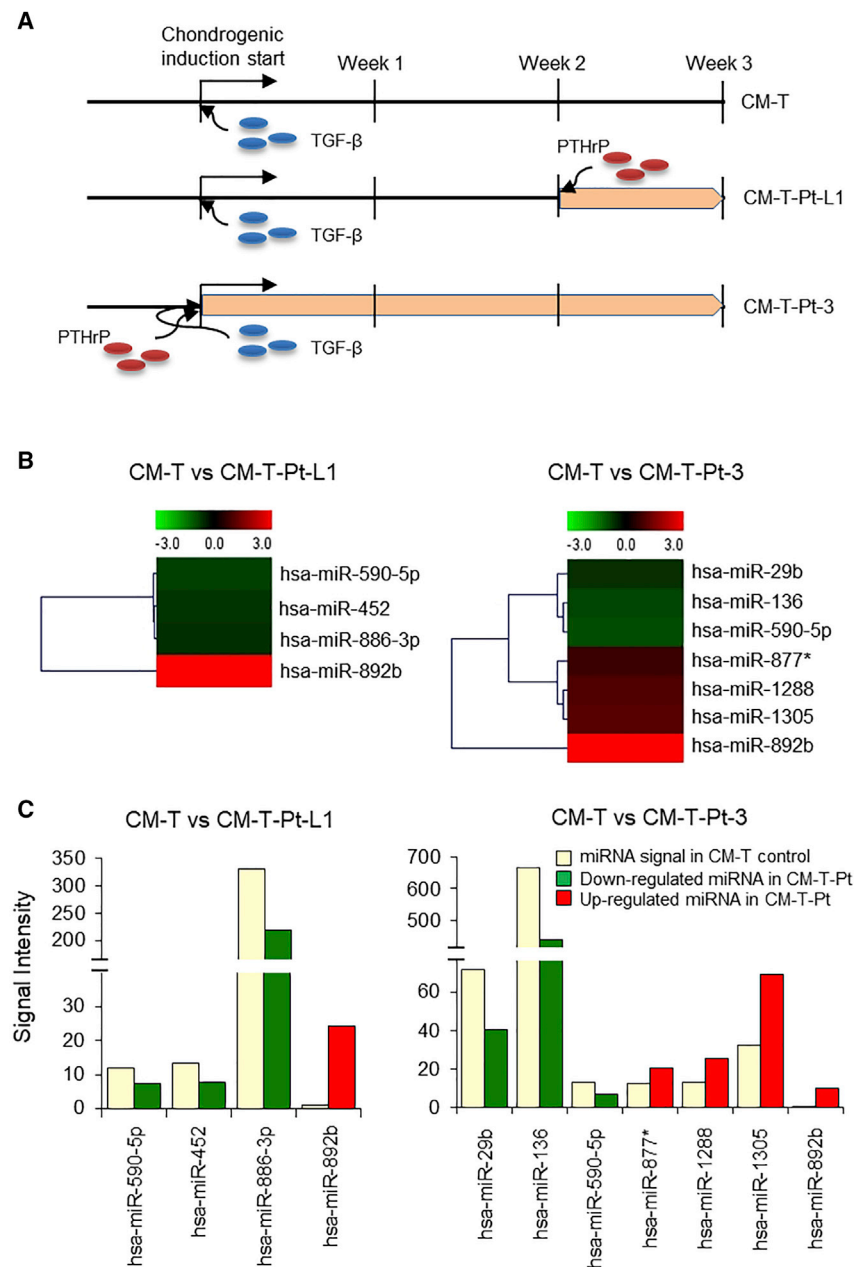


**Figure 1. Inducible Expression of miR-892b by PTHrP Treatment during TGF- $\beta$ -Mediated Chondrogenic Differentiation of hMSCs**

(A) Schematic diagram showing the different start points of PTHrP stimuli during chondrogenic induction of hMSCs. CM-T, chondrogenic medium containing TGF- $\beta$ , and CM-T-Pt-L1, chondrogenic medium containing TGF- $\beta$ , for 3 weeks and PTHrP for the last week only. CM-T-Pt-3, chondrogenic medium containing TGF- $\beta$  and PTHrP for 3 weeks. Expression profiles of various miRNAs in PTHrP-treated groups versus CM-T control. (B) The data were produced by Multi Experiment Viewer (MeV version 4.9). (C) Microarray signal intensities of miRNAs which were up- or downregulated more than 1.5-fold in PTHrP-treated groups versus CM-T control.

(Figures 1A and 1B). Interestingly, hsa-miR-892b expression was not detected in the TGF- $\beta$ -only control. Therefore, PTHrP treatment was critical in hsa-miR-892b expression during TGF- $\beta$ -mediated hMSC chondrogenesis. hsa-miR-892b expression in CM-T-Pt-L1 cells was 2.43-fold higher than that in CM-T-Pt-3 cells (Figure 1C). We also treated PTHrP for the first 3 days of MSC chondrogenic culture in order to confirm the effect of PTHrP treatment at the early stage of chondrogenic differentiation on miR-892b expression. Expression of miR-892b was compared with the untreated control. There was no significant change in the expression level of miR-892b with PTHrP treatment compared with no treatment (Figure S1). Therefore, PTHrP appears to be effective in inducing miR-892b in the latter part of chondrogenic induction, not in the early stage.

**miR-892b Overexpression Mimics PTHrP Function in hMSC Chondrogenesis**

During TGF- $\beta$ -mediated chondrogenic induction of hMSCs, mature miR-892b expression was up-regulated by continuous PTHrP exposure. miR-892b was 2.22-fold ( $p = 0.031$ ) and 2.21-fold ( $p = 0.013$ ) upregulated on days 14 and 21 after

chondrogenic induction, compared with miR-892b expression in untreated cells at the same time points (Figures 2A and 2B).

after PTHrP treatment for the last 1 week (CM-T-Pt-L1) or 3 weeks (CM-T-Pt-3) in TGF- $\beta$ -mediated chondrogenic culture were compared with reference levels obtained from cell pellets treated with TGF- $\beta$  only (CM-T). Under identical chondrogenesis conditions (except for PTHrP treatment), miRNA-expression patterns were relatively unchanged when compared with the TGF- $\beta$ -only control, which simplified the selection of candidate miRNAs. Microarray analysis revealed that only four miRNAs in CM-T-Pt-L1 cells and seven miRNAs in CM-T-Pt-3 cells were differentially expressed after PTHrP treatment. hsa-miR-590-5p and hsa-miR-892b were down-regulated or upregulated respectively in both PTHrP-treated groups

chondrogenic induction, compared with miR-892b expression in untreated cells at the same time points (Figures 2A and 2B).

To investigate the effect of miR-892b overexpression on hMSC chondrogenesis, we constructed a lentiviral vector expressing miR-892b (lenti-miR-892b virus; Figure S2A). hMSCs showed efficient infection by a control virus or lenti-miR-892b at a MOI of 10 (Figure 2C). After chondrogenic induction of each transduced hMSC for 4 weeks (PTHrP treatment in the past 2 weeks), the chondrogenic potential of each pellet was evaluated. Although the gross appearances of chondrogenic pellets in all groups were similar (~0.8–1.0 mm),

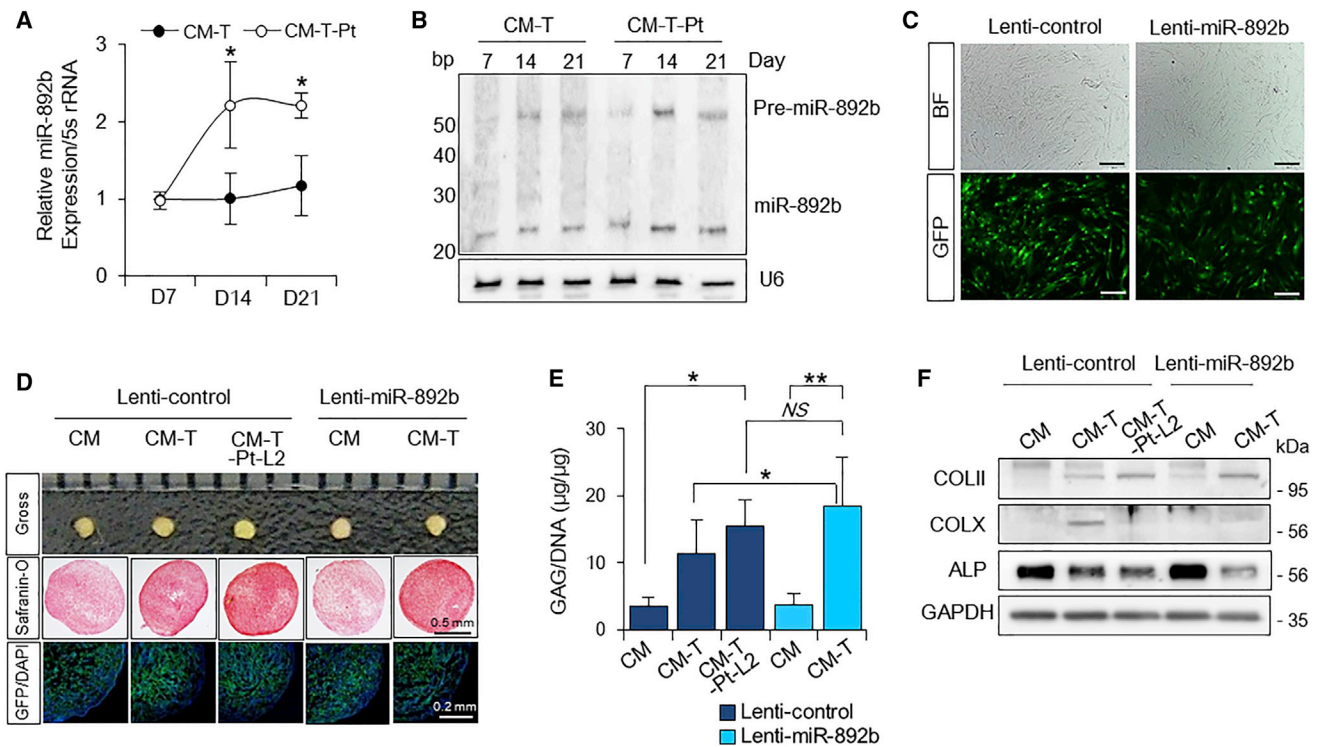


**Figure 2. PTHrP-Induced miR-892b Enhanced Chondrogenesis and Inhibited hMSC Hypertrophy**

Chondrogenic pellets were cultured in CM-T or CM-T-Pt for 7, 14, or 21 days (A and B). (A) qRT-PCR for miR-892b showed that PTHrP stimuli increased miR-892b expression during TGF- $\beta$ -mediated hMSC chondrogenesis (open circles) compared to TGF- $\beta$ -only controls (closed circles). The data are shown as the mean  $\pm$  SD, \* $p$  < 0.05, by paired, two-tailed Student's  $t$  test,  $n$  = 3 donors. (B) Representative northern blot showing expression of mature miR-892b in hMSC chondrogenesis. U6 snRNA was used as a loading control. (C) Fluorescence microscopic images showing the transduction efficiency of lenti-control and lenti-miR-892b viruses into hMSCs. Scale bar, 200  $\mu$ m. (D) Gross appearance, Safranin-O staining, and copGFP expression of pellets were evaluated after 28 days in culture. (E) GAG levels in each pellet were evaluated after normalization to DNA. The data are shown as the mean  $\pm$  SD. \* $p$  < 0.05, \*\* $p$  < 0.01, NS, not significant, by one-way ANOVA followed by the Tukey test,  $n$  = 4 donors. (F) Representative western blot showing chondrogenic and hypertrophic markers from each chondrogenic pellet after 28 days in culture. CM, chondrogenic medium; CM-T, chondrogenic medium containing 10 ng/mL TGF- $\beta$ ; CM-T-Pt, chondrogenic medium containing 10 ng/mL TGF- $\beta$  and 100 ng/mL PTHrP; CM-T-Pt-L2, chondrogenic medium containing 10 ng/mL TGF- $\beta$  and 100 ng/mL PTHrP (PTHrP treatment for the last 14 days only).

Safranin-O pellet staining showed that proteoglycan synthesis was greatest in control lentivirus-transduced chondrogenic pellets when treated with TGF- $\beta$  plus PTHrP. Even without PTHrP, lenti-miR-892b-transduced pellets were similarly stainable compared with control pellets treated with TGF- $\beta$  plus PTHrP (Figure 2D). These effects of miR-892b overexpression were quantified by glycosaminoglycan (GAG):DNA-ratio analysis. The GAG:DNA ratio in lenti-miR-892b-transduced pellets after TGF- $\beta$  treatment increased (63%) over that in control lentivirus-transduced pellets treated with only TGF- $\beta$  and was comparable to control lentivirus-transduced pellets treated with TGF- $\beta$  plus PTHrP (Figure 2E). These findings were validated by investigating the protein expressions of chondrogenic and hypertrophic markers in each pellet. PTHrP treatment increased collagen (COL)2A1 expression and decreased COL10A1 and alkaline phosphatase (ALP) expression, compared with expression levels after TGF- $\beta$  treatment alone, in agreement with previous results.<sup>14</sup> Interestingly, miR-892b overexpression mimicked the effects of PTHrP treatment (Figure 2F). These results indicate that the induced hypertrophy in TGF- $\beta$ -mediated chondro-

genic differentiation of hMSCs can be delayed or prevented by miR-892b, a PTHrP-induced miRNA.

#### miR-892b Targeted KLF10 and Wnt6 in Hypertrophy Signaling

We screened putative miR-892b targets using two miRNA target-prediction databases (Targetscan, [http://www.targetscan.org/vert\\_72/](http://www.targetscan.org/vert_72/), and miRDB, <http://mirdb.org>), followed by analysis with the Database for Annotation, Visualization, and Integrated Discovery (DAVID) Annotation Bioinformatics Database. Chondrocyte hypertrophy is induced through Ihh and Wnt and  $\beta$ -catenin signaling.<sup>15,16</sup> Therefore, it is important to study signals in these pathways that are directly regulated by miR-892b. Specific transcription factors induced by TGF- $\beta$ , which also are direct miR-892b targets and control Ihh expression, can be considered as key regulators of hypertrophy. We selected two candidates, KLF10 and Wnt6, which are involved in hypertrophy signaling and also are miR-892b targets. To confirm that KLF10 and Wnt6 are transcriptionally regulated by miR-892b through interaction with the complementary 3' UTR, luciferase reporters having the 3' UTRs of KLF10 or Wnt6 were constructed



significantly downregulated the mRNA levels of KLF10 (40.26%) and Wnt6 (39.93%) during TGF- $\beta$ -mediated hMSC chondrogenic differentiation. Many signals involved in hypertrophy signaling were also indirectly downregulated by miR-892b overexpression, even if they were not direct targets of miR-892b (Figure 3F). Similarly, downstream proteins of KLF10, Wnt6, and hedgehog (Hh) were reduced by miR-892b overexpression when compared with lenti-control-transduced cells (Figure 3G). These results show that KLF10 and Wnt6 were critical targets of PTHrP-induced miR-892b. However, this does not explain why Ihh and its downstream signals were reduced by miR-892b overexpression. We hypothesized that KLF10 may function as a transcription factor to induce Ihh expression, thereby initiating Hh signaling (Figure 3H).

### KLF10 Is a Transcription Factor Regulating Ihh

To investigate a direct or indirect relationship between KLF10 and Ihh, we constructed an expression plasmid encoding the hKLF10 gene amplified from hMSC cDNA (Figure S2B). Fluorescence-imaging analysis of MSCs transfected with an ECFP control or hKLF10-ECFP plasmid showed that the hKLF10-ECFP fusion protein localized to the nucleus, whereas ECFP was distributed in the cytosol (Figure 4A). Thus, this result indirectly indicates that the recombinant hKLF10 expressed in the MSCs functions like a transcription factor. Then, qRT-PCR analysis was performed with MSC RNA isolated 12 h after transfection. KLF10 mRNA expression in MSCs increased significantly (81-fold) relative to control cells. Ihh mRNA expression increased significantly (12-fold), whereas other downstream signals of Ihh were unaffected. We confirmed that expression of the Ihh protein also increased with the time-dependent increase in KLF10-ECFP fusion proteins (Figures 4B and 4C).

If KLF10 directly regulates Ihh expression as a transcription factor, it should bind to specific sites in the Ihh promoter. Therefore, a sequence containing a 2.0-kb fragment of the 5' flanking region of human Ihh was synthesized and sequenced. The sequence revealed that this region bears three putative SP1/KLF10-binding sites (5'-GGCGGGG-3').<sup>17,18</sup> The +1 nucleotide position indicates an adenine residue of the ATG. The 5'-GGCGGGG-3' sites are located at nucleotides -753 to -747, -710 to -703, and -689 to -683. To characterize the promoter region, we cloned the 2,000-bp, 1,382-bp (-1,382/-1), 1,203-bp (-1,203/-1), 836-bp (-1,203/-367), and 367-bp (-367/-1) fragments and three mutated sequences of the 836-bp fragment into a luciferase expression vector, pGL4, using unique restriction enzyme sites within each sequence. These constructs were co-transfected with pECFP or pECFP-hKLF10 into HEK293 cells. When KLF10 was overexpressed, the pGL4-836 construct, containing bp -1,203 to -367, showed 164% greater transcriptional activity than when co-transfected with the pECFP control vector ( $p < 0.001$ ), whereas other constructs were unaffected by KLF10 overexpression. Interestingly, the promoter activities of the pGL4-2000, 1,382-bp, and 1,203-bp constructs were unchanged, although the putative SP1/KLF10-binding sites were present. Also, the pGL4-836-M1 (-753 to -747) and -M2 (-710 to -703) mutated clones showed less transcriptional activity than when co-transfected with the unmutated

normal pGL4-836 construct (20.6%,  $p = 0.025$ , pGL4-836-M1 versus the wild-type control; 40.6%,  $p < 0.001$ , pGL4-836-M2 versus the wild-type control), whereas mutations in the other SP1/KLF10-binding site did not show significant loss of the promoter activities (Figure 4D).

To determine whether Ihh was directly regulated by KLF10, an electrophoretic mobility shift assay (EMSA) was performed, using biotin-labeled probes containing three putative SP1/KLF10-binding sites. The EMSA showed a significant shift in the binding reactions with probes 1 and 2 after KLF10 overexpression. Probe 2 (but not probe 1) showed an increased intensity of the shifted band after KLF10 overexpression (Figure 4E). We confirmed the specificity of the probe 2-KLF10 complex, using a 200-fold excess of a probe-2 competitor (Figure 4F). In addition, chromatin immunoprecipitation-PCR (ChIP-PCR) results clearly demonstrated that an anti-KLF10 antibody precipitated the 345-bp chromatin region containing the three SP1/KLF10 binding sites (Figure 4G). These results strongly suggest that KLF10 can directly bind at the 5'-<sup>-710</sup>GGCGGGG<sup>-703</sup>-3' elements and plays an important role in mediating the activation of the Ihh promoter.

### Like miR-892b, KLF10 Downregulation Enhances Chondrogenesis and Inhibits hMSC Hypertrophy

We further investigated whether chondrocyte hypertrophy could be directly prevented during long-term hMSC chondrogenesis by KLF10 knock down (KD) using with short-hairpin RNA (shRNA). KLF10 mRNA and protein expression were effectively downregulated by lentiviral transduction of hMSCs (MOI = 20) with shRNA clone 2 (Figure 5A and S2C). After a 4-week induction of chondrogenesis in lentiviral-transduced hMSCs in the presence of TGF- $\beta$ , the chondrogenic potential of each pellet was analyzed. Safranin-O pellet staining showed that KLF10 KD enhanced proteoglycan synthesis (Figure 5B). qRT-PCR results showed that Col2A1 mRNA in lenti-shK-C2-transduced pellets increased significantly (1.77-fold) versus that in lenti-control pellets, whereas SOX9 mRNA induction was not significant. Moreover, KLF10 KD, like miR-892b, decreased the mRNA expression of hypertrophic markers. The mRNA level of Col10a1, a representative hypertrophic marker of chondrocytes, decreased by 41%, whereas Alpl expression decreased by 54%, (Figure 5C). Also, protein expression followed the patterns of gene expression (Figure 5D). In addition, we observed which signal molecules in Ihh and Wnt and  $\beta$ -catenin signaling were affected by KLF10 KD. qRT-PCR showed that KLF10 shRNA decreased KLF10 mRNA by 43%, which resulted in decreased mRNA expression of Ihh (55%), Ptch1 (47%), Smo (52%), Wnt3a (44%), and Ctnnb1 (51%). Unlike miR-892b, the mRNA levels of Ptch2, Gli-2, Wnt7a, Wnt6, and Wnt9b were unaffected by KLF10 KD. The protein expression levels also agreed with the qRT-PCR results (Figures 5E and 5F). Together, these data suggest that KLF10 is critical for initiation of hypertrophy during TGF- $\beta$ -mediated chondrogenesis of hMSCs and that repressed KLF10 expression induces the enhanced chondrogenesis of hMSCs through downregulation of Ihh and  $\beta$ -catenin.

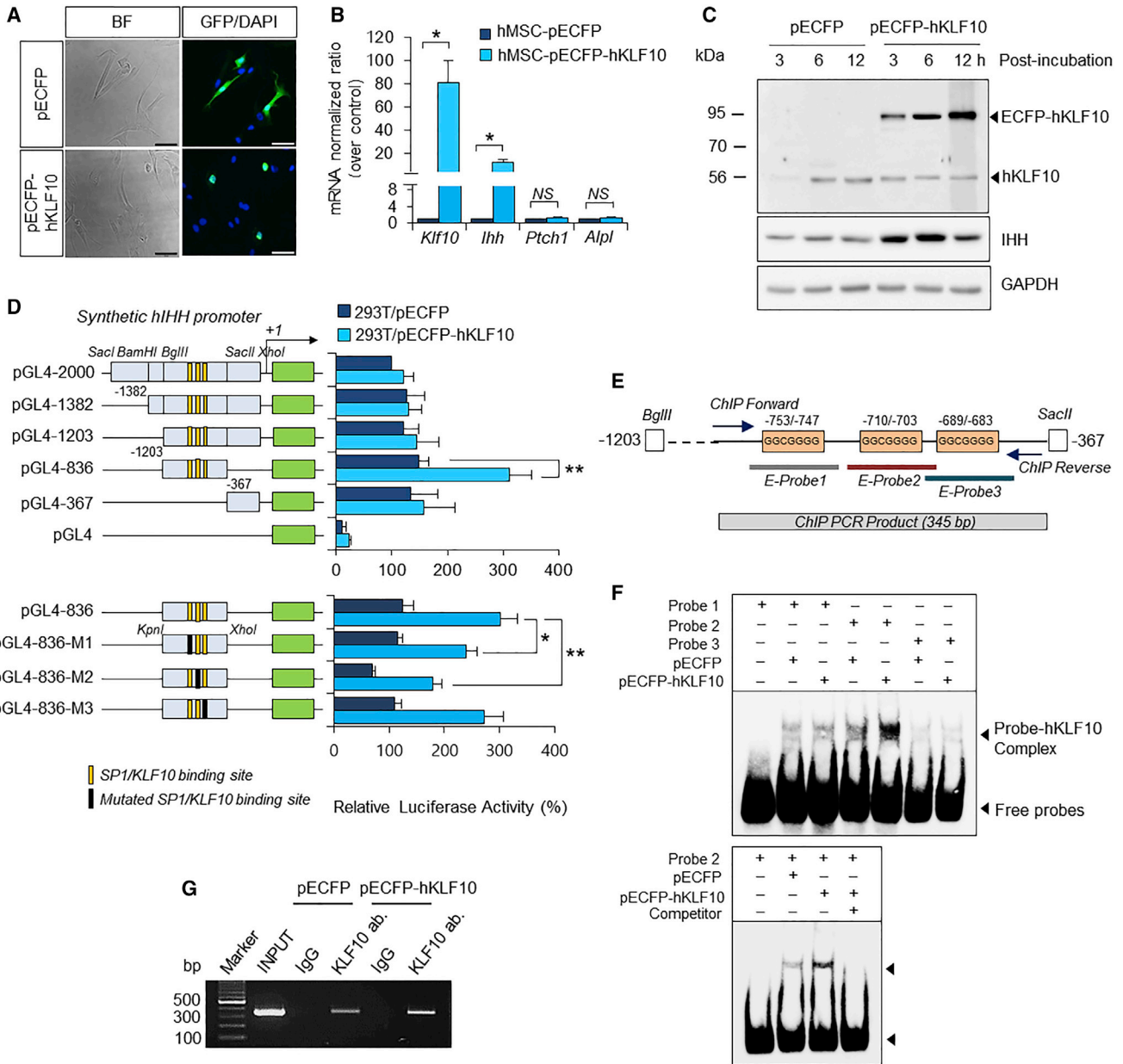


**Figure 4. KLF10 Directly Regulates Human *Ihh* Expression through Binding to the SP1/KLF10 Sites in Its Promoter**

(A) Transient expression of rhKLF10 in hMSCs. The ECFP-hKLF10 fusion protein translocated to the nucleus. Scale bars, 50  $\mu$ m. (B) rhKLF10 and *Ihh* expression and downstream signals at 12 h after transfection. Data are shown as the mean  $\pm$  SD. \* $p < 0.05$ , NS, not significant, by Mann-Whitney U test,  $n = 4$  donors. (C) Representative western blot showing KLF10 and *Ihh* expression from hMSCs at 3, 6, and 12 h. (D) Reporter gene assay using pGL4 constructs containing different synthetic *Ihh* promoters and the pECFP control, or the pECFP-hKLF10 expression vector in HEK293T cells. The three yellow boxes in the promoter sequence represent SP1/KLF10 binding sites. The black box represents the position of the mutated SP1/KLF10 binding site. Data are shown as the mean  $\pm$  SD. \* $p < 0.05$ , \*\* $p < 0.01$ ,  $n = 5$  independent experiments, by paired, two-tailed Student's *t* test in comparison with wild-type promoter fragments, one-way ANOVA followed by the Tukey test in comparison with the mutated clones. (E) Schematic of three probe sites for EMSA and the template region for ChIP-PCR analysis within the 836-bp *Ihh* promoter. Primers for ChIP-PCR were designed using the Primer-BLAST tool. (F) Binding of the designed three SP1/KLF10 probes and nuclear extracts from HEK293T cells transfected with pECFP control or pECFP-hKLF10 for 12 h. (G) ChIP-PCR was performed after 12 h of transfection. ChIP-PCR of the nuclear extracts precipitated using anti-KLF10 antibody or a control rabbit IgG.

## DISCUSSION

miR-892b has been identified as a tumor suppressor that attenuates NF- $\kappa$ B signaling.<sup>19</sup> However, the functional role of miR-892b during MSC differentiation is unclear. Here, we demonstrated that miR-892b inhibits hypertrophy induced during TGF- $\beta$ -mediated MSC chondrogenesis. We propose that the negative-feedback inhibition of Ihh by PTHrP can be induced through KLF10 suppression.

KLF10 and Wnts are transcriptionally expressed after nuclear translocation of the Smad2/3 and Smad4 complex activated by TGF- $\beta$  signal.<sup>20,21</sup> In addition to causing Smad7 downregulation to maintain activated TGF- $\beta$ /Smad signaling,<sup>22</sup> our results showed that KLF10 can mediate novel cross-talk between TGF- $\beta$ /Smad and Hh signaling by directly activating the Ihh promoter (Figure 6A). This cross-talk provides critical clues explaining the lack of osteoblast markers and reduced bone mineralization in osteoblasts from KLF10 KO mice.<sup>23</sup> After Ihh is upregulated by the transcriptional activity of KLF10 and secreted from the cells, this Ihh ligand can activate Hh signaling, resulting in Ptch inhibition, Smo release from Ptch, and Gli activation. Finally, the activated Gli upregulates target genes involved in chondrocyte hypertrophy during TGF- $\beta$ -mediated MSC chondrogenesis.<sup>15</sup>

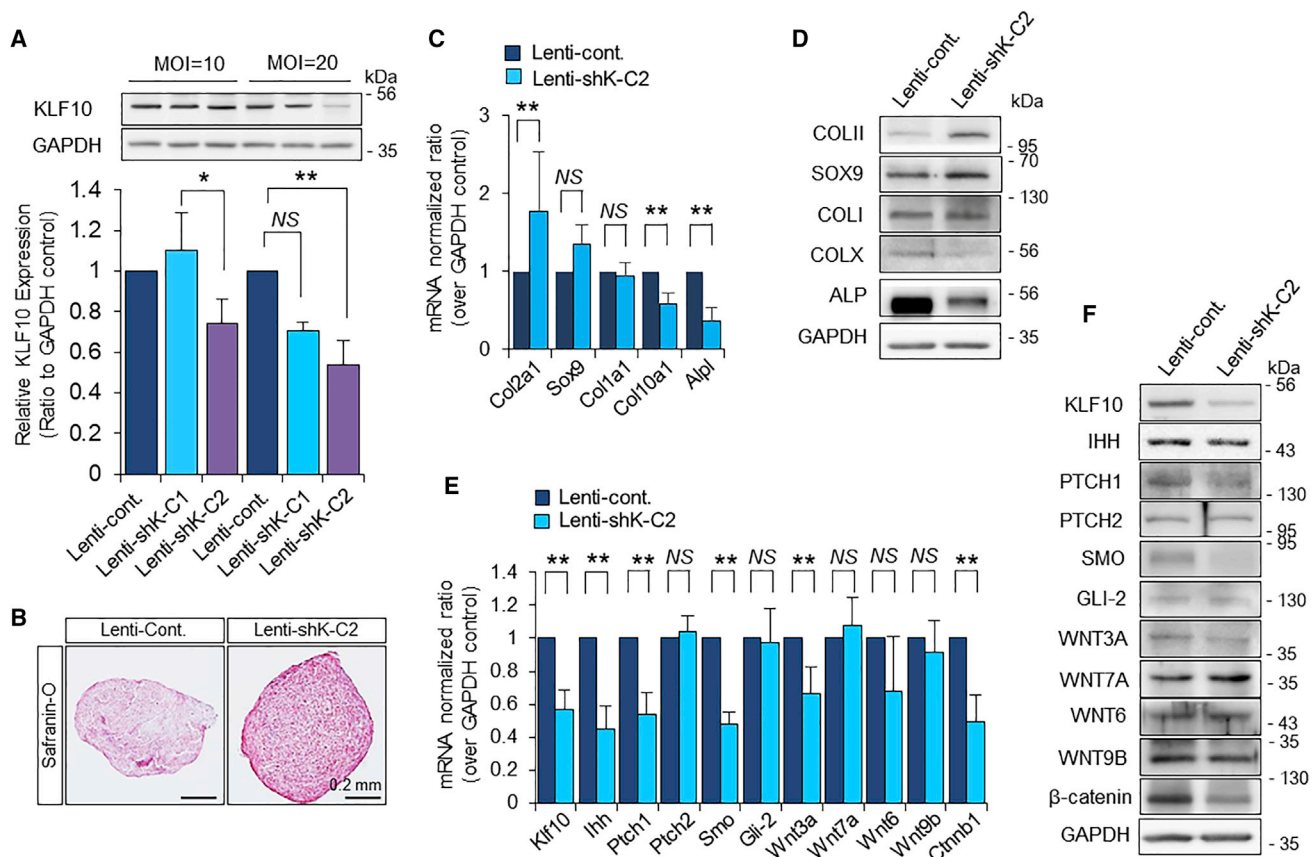
During endochondral bone development, Ihh in the hypertrophic chondrocyte zone can increase PTHrP expression by Gli2 activation during the mTORC1/S6K1 cascade.<sup>24</sup> Conversely, in immature chondrocytes, which are found in both the resting and columnar zones of the growth plate, PTHrP induces protein kinase A (PKA) activity to promote histone deacetylase 4 (HDAC4) dephosphorylation. Dephosphorylated HDAC4 in the nucleus inhibits the activity of the Mef2 and Runt-related transcription factor (Runx) family members, thereby blocking chondrocyte hypertrophy.<sup>25,26</sup> Our data showed a novel miRNA-based regulation mechanism present in the PTHrP and Ihh negative-feedback loop. Although it is unclear which signal(s) upregulates miR-892b expression, the signal can be predicted based on its chromosomal position. Although some miRNAs are co-transcribed with host genes,<sup>27,28</sup> most are transcribed as independent units.<sup>10,29</sup> miR-892b may be transcribed independently with its own promoter, considering that no host gene is located near its location in the chromosome. Based on the well-documented mechanism of miRNA biogenesis,<sup>30</sup> after pri-miR-892b is transcribed by an unknown signal in the PTHrP signaling cascade, pre-miR-892b would be generated from pri-miR-892b by Drosha. After pre-miR-892b translocates to the cytosol, Dicer would process it again to the mature miR-892b. Mature miR-892b would induce KLF10 mRNA degradation by forming an RNA-induced silencing complex, causing suppression of Ihh and hypertrophic signals (Figure 6B).

It has been reported that upregulated Ihh signaling in chondrocytes can induce hypertrophy of chondrocytes by activating the expression of some Wnt ligands and subsequent canonical Wnt signaling.<sup>31</sup> Recently, it was reported that KLF10 not only regulates the expression of various Wnt ligands during osteogenesis but also induces nuclear translocation of  $\beta$ -catenin or contributes to their stabilization.<sup>32</sup>

Conversely, inhibition of Ihh by KLF10 KD or miR-892b expression during chondrogenic differentiation of hMSCs can cause inhibition of some Wnt signals and  $\beta$ -catenin. Although KLF10 shRNA and miR-892b were expressed in hMSCs by using a common tool, lentiviral transduction, it is not easy to determine which one of them has a greater impact on regulation of Wnt ligands and downstream signals, because the type of two viral vectors used for lentivirus production and the viral-infection conditions into hMSCs are different. However, miR-892b targets a variety of mRNAs that can regulate hypertrophic chondrocyte maturation in addition to KLF10. Therefore, miR-892b might be more effective for suppressing chondrocyte hypertrophy than KLF10 shRNA.

Wnt signaling can influence cross-talk between cartilage and subchondral bone.<sup>16</sup> During late embryonic and postnatal development, trabecular bone formation is strongly dependent on  $\beta$ -catenin expression in chondrocytes in the lower hypertrophic zone. Wnt proteins are key regulators of bone, cartilage, joint development, and homeostasis.<sup>33–36</sup> Wnt6 inhibits chondrogenesis upstream of Sox9 and type II collagen expression in chick embryos and blocks adipogenesis and stimulates osteoblastogenesis.<sup>37,38</sup> We showed that miR-892b could directly bind to the 3' UTR of Wnt6 mRNA and that Wnt6 expression decreased in chondrogenic pellets of lenti-miR-892b-transduced MSCs. Interestingly, other Wnts were also downregulated, even though their 3' UTR lacks a miR-892b-binding site. Wnt3a induces chondrocyte hypertrophic maturation and bone formation.<sup>39</sup> Wnt7a suppresses chondrogenic differentiation in a high-density chick limb bud cell culture model.<sup>40</sup> We confirmed that endogenous Wnt3a and Wnt7a expression decreased in chondrogenic pellets expressing miR-892b. This finding suggests the possibility that miR-892b also promotes chondrogenesis and inhibits hypertrophy by suppressing Wnt signal in MSC chondrogenesis. In addition,  $\beta$ -catenin, a nuclear effector of Wnt and  $\beta$ -catenin signaling, may also be a target gene because computational miRNA target prediction suggests the presence of a binding site on miR-892b at nucleotide position 29–35 within its 3' UTR. Chondrogenic differentiation in micromass cell culture was extensively enhanced by  $\beta$ -catenin inactivation. Weakened canonical Wnt signaling results in reduced bone density.<sup>41,42</sup> Importantly, we found that  $\beta$ -catenin was downregulated in MSCs expressing miR-892b or KLF10 shRNA during TGF- $\beta$ -mediated chondrogenesis.

KLF10 was initially identified in normal human fetal osteoblasts after TGF- $\beta$  treatment.<sup>43</sup> KLF10 binds to GC-rich, Sp1-like sequences of target promoters to regulate downstream gene transcription.<sup>17,44</sup> Fifty-eight percent of the 2 kb-sequence upstream of the transcription start site of human Ihh is composed of GC. Because cloning GC-rich genes from genomic DNA generally has a very low success rate, we used a synthetic Ihh promoter to verify whether the promoter directly interacted with KLF10. Reporter gene analysis, using the synthetic Ihh promoter, revealed that KLF10 showed increased transcriptional activity only at a specific promoter region (–1,203/–367). Of note, the promoter activities of several constructs containing various upstream base pair regions, plus all the putative KLF10-binding sites,



exhibited no change in response to KLF10 overexpression. We presume that a domain responsible for the suppressing KLF10 action during the chondrogenic differentiation may be present in the  $-2,000$ - to  $-1,203$ -bp region of the *Ihh* promoter. This possibility needs to be further investigated in a future study.

Decisively, EMSA and ChIP analysis clearly showed which of the three 5'-GGCGGGG-3' elements served as a KLF10-binding site. Runx2 can directly activate the mouse *Ihh* promoter,<sup>45</sup> and KLF10 can activate Runx2 expression through its proximal promoter region.<sup>46</sup> Thus, KLF10 may indirectly stimulate *Ihh* expression upstream of Runx2, directly bind the *Ihh* promoter, and activate *Ihh* expression.

To summarize, we identified a novel regulatory mechanism comprising miR-892b and KLF10. It is suggested that KLF10 is a transcription factor controlling *Ihh* promoter activity and that

KLF10 inhibition enhances chondrogenesis and inhibits hypertrophy in MSCs. Our findings present new insights into the transcriptional network system of skeletal development and provide a novel strategy for cartilage tissue engineering.

## MATERIALS AND METHODS

### Cell Culture

The bone marrow samples used to isolate MSCs were obtained from 10 patients (mean age: 49 years; range: 41–58 years) undergoing total hip replacement, due to osteoarthritis. Informed consent was obtained from all donors. This study was approved by the Institutional Review Board (IRB) of Dongguk University Ilsan Hospital (DUIH). MSCs were isolated from fresh bone marrow samples and then expanded as described previously.<sup>4,14,47</sup> The MSCs were authenticated by cell surface markers and cell differentiation assay. Additional hMSCs (Lonza, Basel, Switzerland; CEFO bio, Seoul, Korea) were cultured for *in vitro* analysis according to the manufacturer's



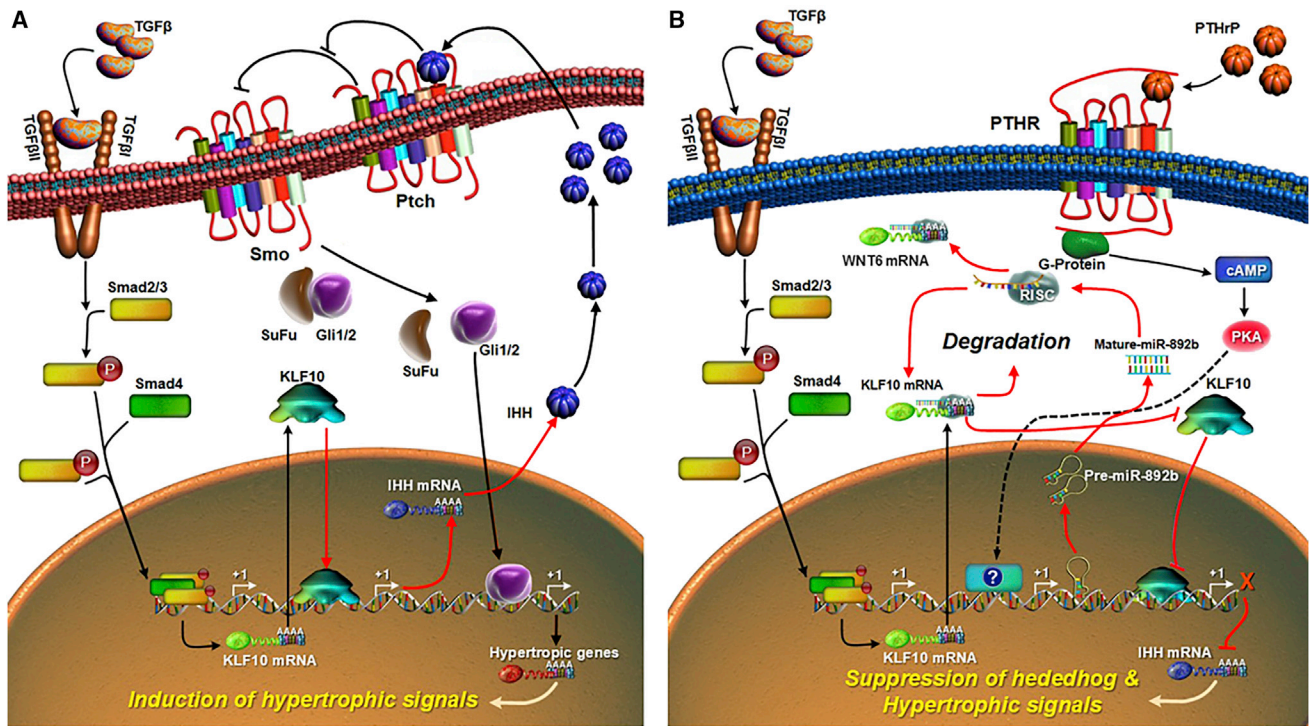


**Figure 6. Roles of KLF10 in Inducing Hypertrophic Signals and Inhibition of KLF10 Via PTHrP-Induced miR-892b**

(A and B) Schematic model depicting the role of KLF10 in *Ihh* upregulation (A) and the inhibition of KLF10-dependent hypertrophic signals by miR-892b (B). The black arrow indicates the previously published pathway, and the red arrow indicates the new pathway was derived from the present study. These pathways were depicted with ePath 3D 1.0 tool (PROTEIN LOUNGE).

instructions. HeLa (ATCC, Manassas, VA, USA), 293FT (Thermo Scientific, Waltham, MA, USA), and HEK293T (ATCC) cells were cultured in DMEM-high glucose (Corning, Corning, NY, USA) supplemented with 10% fetal bovine serum (FBS; Thermo Scientific) and 1% streptomycin and penicillin, in 5% CO<sub>2</sub> at 37°C. All cell lines were routinely tested for mycoplasma contamination and were negative.

#### miRNA Microarray Assay and Computational miRNA Target Prediction

hMSC cell pellets were cultured in chondrogenic medium (CM) containing 10 ng/mL TGF-β3 for 3 weeks. PTHrP stimuli were maintained during all 3 weeks, only during the last week of the 3-week cultivation, only during first 3 days, or not at all. After total RNA was isolated from the cell pellets, the miRNA microarray assay was performed by e-biogen (Seoul, Korea), a microarray agency. miRNA labeling and hybridization was then performed using the miRNA Labeling Reagent and Hybridization Kit (Agilent, Santa Clara, CA, USA). Cy3-labeled samples were then hybridized overnight at 56°C on an Agilent Human miRNA 8 × 15K (V3.0) microarray, which contains probes for 15,000 human miRNAs. Feature-extraction software (Agilent) was used to analyze the scanned images using default parameters to obtain background-subtracted and spatially de-trended processed signal intensities as the raw data. The raw data were normalized in a quantile algorithm with GeneSpring

software (Agilent). Three different databases (MicroCosm Targets, Targetscan, and miRDB) were used to identify potential hsa-miR-892b target genes.

#### Construction of Lentiviral and Non-viral Expression Plasmids

A 341-bp pri-miRNA sequence corresponding to hsa-miR-892b was amplified from the genomic DNA of hMSCs using a specific primer pair (Figure S2A; Table S1). The amplified pri-hsa-miR-892b sequence was then inserted into the pGEM-T-Easy vector (Promega, Madison, WI, USA), after which the NheI-EcoRI fragment containing pri-miR-892b was ligated into the multi-cloning site of the pCDH-copGFP vector (System Biosciences, Palo Alto, CA, USA) to yield pCDH-miR-892b-copGFP. For human KLF10 overexpression, total RNA from hMSCs was isolated using an RNeasy Mini Kit (QIAGEN, Hilden, Germany), according to the manufacturer's instructions, and the RNA was converted to cDNA, using the QuantiTect Reverse Transcription Kit (QIAGEN). The hKLF10 open reading frame was amplified with a specific primer pair (Figure S2B; Table S1), subcloned into the pGEM-T-Easy vector, and cloned between the BglII and SalI sites of the pECFP-C1 vector (Clontech, Mountain View, CA, USA). For the KLF10-KD study, 5' and 3' single-stranded oligonucleotides corresponding to human KLF10 shRNAs were designed using the BLOCK-iT RNAi Designer (Thermo Scientific) and synthesized. After these complementary oligonucleotides were annealed, the

double-stranded oligonucleotides were ligated between the AgeI and EcoRI sites of the pLKO.1-Puro vector (Addgene, Cambridge, MA, USA) (Figure S2C; Table S1). All pGEM-T-Easy vectors ligated with PCR products in this work were verified by DNA sequencing.

#### Lentiviral Transduction and Induction of *In Vitro* Chondrogenic Differentiation

293FT cells were co-transfected with lentiviral vector constructs and the lentiviral packaging mixture (pLP1, pLP2, and pLP/VSVG; Thermo Scientific) to produce the corresponding lentiviruses. At 48 h after transfection, viral supernatants were collected and stored at  $-80^{\circ}\text{C}$  until use. MSCs at passage 3 were seeded into six-well plates or 10-cm dishes and then transduced with lentiviral supernatant for 7 h in the presence of polybrene (8  $\mu\text{g}/\text{mL}$ ; Sigma-Aldrich, St. Louis, MO, USA) at different MOIs. When the confluence of the lentiviral vector-transduced MSCs reached approximately 80%, the cells were trypsinized, and chondrogenesis was induced at passage 4. Chondrogenic induction of the lentiviral vector-transduced MSCs was performed as described previously.<sup>47</sup> After 4 weeks of *in vitro* culture, chondrogenic pellets were harvested for analysis. In MSCs showing insignificant changes of chondrogenic markers in the positive control group (TGF- $\beta$  only treated) versus the negative control group after chondrogenic culture, results obtained from the cells were excluded in the process of data production.

#### qRT-PCR Analysis

Total RNA for mRNA qRT-PCR analysis was isolated using an RNeasy Mini Kit (QIAGEN), according to the manufacturer's instructions, and quantified using an IMPLEN Nanophotometer P330. Isolated RNA samples were converted to cDNA with a QuantiTect Reverse Transcription Kit (QIAGEN). All PCR was performed using a QuantiTect SYBR Green PCR Kit (QIAGEN) and a Rotor-Gene Q (QIAGEN) in standard 15- $\mu\text{L}$  reactions. The amplification primers and their target mRNAs are shown in Table S2. All samples were processed in triplicate to increase the reliability of the results obtained. Each assay was performed using positive and negative controls. The threshold cycle ( $C_t$ ) value of each gene was measured for each sample. The  $C_t$  value of glyceraldehyde-3-phosphate dehydrogenase (GAPDH) was used as an endogenous reference for normalization purposes. The values thus obtained were normalized versus the negative control and expressed as fold changes. To quantify hsa-miR-892b expression, total RNA was extracted using TRIzol (Thermo Scientific), converted into cDNA, and amplified with the GenoExplorer miRNA qRT-PCR Kit (GenoSensor, Tempe, AZ, USA), according to the manufacturer's instructions. A hsa-miR-892b specific primer and a universal reverse primer provided by the manufacturer were used to amplify hsa-miR-892b, and the  $C_t$  value of 5 s rRNA was used as an endogenous control for normalization.

#### Northern Blot Analysis of miRNA Expression

For northern blot analysis of miRNA expression, 10  $\mu\text{g}$  of total RNA was separated on 15% denaturing polyacrylamide gels, electrotransferred onto nylon membranes (GE Healthcare, Buckinghamshire,

UK), cross-linked with UV light, and baked for 1 h at  $80^{\circ}\text{C}$ . A biotin-labeled locked nucleic acid (LNA) probe (Exiqon, Woburn, MA, USA), complementary to the mature miR-892b, was hybridized overnight at  $42^{\circ}\text{C}$  in ULTRAHYB buffer (Thermo Scientific). The LNA probe sequence is shown in Table S2. The blots were washed in  $2\times$  saline sodium citrate (SSC) and 0.1% SDS and in  $0.1\times$  SSC and 0.1% SDS at  $42^{\circ}\text{C}$ , and detected with the Chemiluminescent Nucleic Acid Detection Module (Thermo Scientific) and LAS-3000 (FUJIFILM, Valhalla, NY, USA). U6 snRNA was used as a loading control.

#### DNA Quantification and GAG Contents Analysis

Chondrogenic pellets were digested for 2 h at  $56^{\circ}\text{C}$  in cell lysis buffer containing proteinase K from the GeneAll Tissue SV Mini Kit (GeneAll Biotech, Seoul, Korea). Next, genomic DNA from each pellet was prepared according to the manufacturer's instruction. DNA contents were determined using an IMPLEN nanophotometer P330 (Implen, Munich, Germany). To analyze GAG contents, pellets were digested in papain buffer at  $60^{\circ}\text{C}$  for 2 h, and GAG production was determined using a Blyscan Kit (Biocolor, County Antrim, UK), according to the manufacturer's instructions. Absorbance was measured at 656 nm in a Spectra Max Plus 384 (Molecular Devices, Sunnyvale, CA, USA). GAG contents were expressed as the number of micrograms of GAG per microgram of DNA.

#### Western Blot Analysis

For total protein extraction, pellets washed twice with cold PBS were homogenized by grinding in  $\text{LN}_2$  and incubated with radioimmunoprecipitation assay (RIPA) cell lysis buffer supplemented with Halt protease and phosphatase inhibitor cocktail (Thermo Scientific) for 30 min on ice, and centrifuged at 15,000 rpm for 20 min at  $4^{\circ}\text{C}$ . Proteins were separated by SDS-PAGE on an 8%–10% separating gel, electroblotted onto a polyvinylidene difluoride membrane, and blocked for 1 h in 5% non-fat dry milk in PBS or TBS containing 0.05% Tween 20 (PBS-T or TBS-T, respectively). Subsequently, the membranes were incubated with appropriate primary antibodies overnight at  $4^{\circ}\text{C}$ . Next, the membranes were washed three times with PBS-T or TBS-T and then incubated with horseradish-peroxidase-labeled anti-mouse or anti-rabbit IgG (1:3,000; Abcam, Cambridge, UK) for 1 h at room temperature. After a further wash step, bands were visualized using the ECL+Plus Western Blotting System (GE Healthcare). Antibodies corresponding to the target proteins are described in Table S3. The Western band was quantified using the ImageJ program, normalized to the GAPDH band, and statistically processed (Figure S3).

#### Transient Expression of Human KLF10 and the Luciferase Reporter Assay

Subconfluent MSCs were harvested and washed with PBS. MSCs were resuspended in resuspension buffer R (Thermo Scientific) at a density of  $2 \times 10^6$  cells per 100  $\mu\text{L}$  and mixed with 5  $\mu\text{g}$  of the pECFP or pECFP-hKLF10 plasmid. Then, electroporation was performed with a Microporator (Thermo Scientific) using an optimized program (1,300 V, 30 ms, and 1 pulse). After electroporation, the cells were

plated in a six-well plate and placed in 37°C in 5% CO<sub>2</sub>. The cyan fluorescence of ECFP was visualized with a DMI 6000B microscope (Leica Microsystems, Wetzlar, Germany). Total proteins were harvested from cell lysates at 6, 12, and 24 h after transfection and used for western blot analysis. Total RNAs were also isolated for qRT-PCR analysis at 12 h after transfection. For each reporter gene assay, cells were seeded the day before transfection into 24-well plates (0.5 × 10<sup>5</sup> cells per well for HeLa cells and 1.5 × 10<sup>5</sup> cells per well for HEK293T cells). For the 3' UTR reporter gene assay to identify putative miR-892b target genes, 5' and 3' single-stranded oligonucleotides corresponding to the WT (WT-3' UTR) or mutant (MUT-3' UTR) miR-892b binding site in the UTR of KLF10 (NM\_005655) or WNT6 (NM\_006522) were synthesized, respectively. After each oligo was annealed, the double-stranded oligonucleotides were ligated between the SpeI and HindIII restriction sites of the pMIR-REPORT vector (Thermo Scientific). The oligonucleotides sequences are presented in Table S2. For the luciferase assays, HeLa cells were transfected with 500 ng of the above constructs and co-transfected with 50 nM miR-892b mimic or negative-miR control (Dharmacon, Lafayette, CO, USA), using the X-tremeGENE siRNA-transfection reagent, according to the manufacturer's protocol (Roche). For a reporter gene assay with the Ihh promoter, a region -2 kb upstream of the transcription start site of Ihh (NG\_016741.1) was synthesized (Thermo Scientific), and its different fragments were ligated into the pGL4 reporter plasmid (Promega), as shown in Figure 3D. An 836-bp fragment containing three predicted SP1/KLF10 binding sites, 5'-GGCGGGG-3', were synthesized for converting to three mutated fragments, 5'-GGATGGG-3', and the mutated fragments were ligated into the pGL4 plasmid (Figure S4). Cells were co-transfected with each pGL4 plasmid (500 ng) encoding the firefly luciferase gene controlled under different fragments of the Ihh promoter and the pECFP empty vector or pECFP-hKLF10 vector (500 ng) using the X-tremeGENE HD transfection reagent. At 24 h after transfection, luciferase activities were quantified in whole-cell lysates by using the Luciferase Reporter Assay System (Promega), according to the manufacturer's protocol. Measurements were performed on an FB 12 Luminometer (Berthold, Wildbad, Germany). In each experiment, luciferase activities were normalized to the amount of lysate protein and expressed relative to that in cell transfected with a negative-control miRNA (3' UTR assay) or pGL4-2k Ihhpro and pECFP co-transfection (Ihh promoter assay). Each value was calculated as the mean of the results from five wells, and each experiment was repeated five times.

#### EMSA

Nuclear extracts from HEK293T cells transfected with a pECFP control or pECFP-hKLF10 vector for 12 h were prepared with the Nuclear Extract Kits (Origene, Rockville, MD, USA). Protein concentrations were determined using the BCA Protein Assay Kit (Bio-Rad, Hercules, CA, USA). Oligonucleotides containing SP1/KLF10 binding sites were synthesized (Table S2). Single-stranded oligonucleotides were 3' end labeled with biotin, using a Biotin 3' End DNA-Labeling Kit (Thermo Scientific) according to the manufacturer's protocol, and were annealed to obtain double-stranded DNA probes.

To reduce non-specific binding, nuclear extracts (8 µg) were pre-incubated with 5× binding buffer (100 mM HEPES [pH 7.9], 250 mM KCl, 25% glycerol), 0.1 mM EDTA, 200 µg/mL BSA (fraction V [FV] grade) containing 1 mM DTT, and 1 µg Poly (dI·dC) for 20 min at 4°C. Then 20 fmol biotin-labeled DNA probe was added to the mixture and post incubated for 1 h at 4°C. Protein-DNA complexes were separated by 5% native PAGE and transferred to a positively charged nylon membrane. Cross-linking was performed under UV light for 20 min, and then the biotin-labeled DNA was detected using the Chemiluminescent Nucleic Acid Detection Module (Thermo Scientific). For competition experiments, unlabeled competitor oligonucleotides were post incubated (200-fold excess) with the labeled probe.

#### ChIP Experiments

Chromatin was prepared for the ChIP assay using the EZ-Zyme Chromatin Prep Kit (EMD Millipore, Billerica, MA, USA) according to the manufacturer's protocol. Approximately 4 × 10<sup>7</sup> HEK293T cells were cross-linked in 1% formaldehyde at room temperature for 10 min before terminating the cross-linking reaction with glycine. The cells were collected and resuspended in ChIP lysis buffer (50 mM HEPES [pH 7.5], 140 mM NaCl, 1 mM EDTA [pH 8.0], 1% Triton X-100, 0.1% sodium deoxycholate, and 0.1% SDS) containing protease inhibitors (Thermo Scientific) for further sonication to shear the chromatin with a 200- to 1,500-bp smear. DNA-protein complexes (25 µg) were immunoprecipitated with anti-KLF10 antibodies (GeneTex, Irvine, CA, USA) or a control rabbit polyclonal anti-IgG antibody (Abcam). DNA-protein cross-linkers were reversed by heating at 65°C for 4 h. DNA products were precipitated with ethanol after performing an RNase A and proteinase K reaction, followed by two successive phenol extractions. The DNA products were used as a template for PCR, and primers (Table S2) were used to amplify a 345-bp promoter region of human Ihh. Each experiment was repeated three times.

#### Statistics and Reproducibility

Descriptive statistics were used to determine the group means and standard deviations of numerical data; Student's t test (unpaired, two-tailed) and the Mann-Whitney U were used test to compare differences between two groups; and one-way ANOVA, followed by Tukey correction, was used for multiple comparisons. *p* < 0.05 was considered significant. In each experiment, the sample size was determined on the basis of our prior knowledge of the variability of experimental output. The number of biological (non-technical) replicates for each experiment is indicated in the figure legends.

#### SUPPLEMENTAL INFORMATION

Supplemental Information can be found online at <https://doi.org/10.1016/j.omtn.2019.05.029>.

#### AUTHOR CONTRIBUTIONS

J.M.L., J.-Y.K., H.Y.K., and J.-W.P. performed the experiments and analyzed the data. J.M.L. and G.-I.I. designed the experiments and wrote the manuscript. F.G. provided technical assistance and edited the manuscript.

## CONFLICTS OF INTEREST

The authors declare no competing interests.

## ACKNOWLEDGMENTS

This study was supported by a grant from the Korea Health Technology R&D Project through the Korea Health Industry Development Institute (KHIDI), funded by the Ministry of Health & Welfare, Republic of Korea (HI18C2186) and the National Research Foundation of Korea (NRF-2019R1H1A2039685 and 2016R1C1B1008616).

## REFERENCES

- Mueller, M.B., and Tuan, R.S. (2008). Functional characterization of hypertrophy in chondrogenesis of human mesenchymal stem cells. *Arthritis Rheum.* 58, 1377–1388.
- Mueller, M.B., Fischer, M., Zellner, J., Berner, A., Dienstknecht, T., Prantl, L., Kujat, R., Nerlich, M., Tuan, R.S., and Angele, P. (2010). Hypertrophy in mesenchymal stem cell chondrogenesis: effect of TGF- $\beta$  isoforms and chondrogenic conditioning. *Cells Tissues Organs* 192, 158–166.
- Im, G.I., Kim, H.J., and Lee, J.H. (2011). Chondrogenesis of adipose stem cells in a porous PLGA scaffold impregnated with plasmid DNA containing SOX trio (SOX-5, -6 and -9) genes. *Biomaterials* 32, 4385–4392.
- Kim, H.J., and Im, G.I. (2011). Electroporation-mediated transfer of SOX trio genes (SOX-5, SOX-6, and SOX-9) to enhance the chondrogenesis of mesenchymal stem cells. *Stem Cells Dev.* 20, 2103–2114.
- Lee, J.M., and Im, G.I. (2012). SOX trio-co-transduced adipose stem cells in fibrin gel to enhance cartilage repair and delay the progression of osteoarthritis in the rat. *Biomaterials* 33, 2016–2024.
- Fischer, J., Dickhut, A., Rickert, M., and Richter, W. (2010). Human articular chondrocytes secrete parathyroid hormone-related protein and inhibit hypertrophy of mesenchymal stem cells in coculture during chondrogenesis. *Arthritis Rheum.* 62, 2696–2706.
- Yang, Y.H., Lee, A.J., and Rababino, G.A. (2012). Coculture-driven mesenchymal stem cell-differentiated articular chondrocyte-like cells support neocartilage development. *Stem Cells Transl. Med.* 1, 843–854.
- Ahmed, M.R., Mehmood, A., Bhatti, F.U., Khan, S.N., and Riazuddin, S. (2014). Combination of ADMSCs and chondrocytes reduces hypertrophy and improves the functional properties of osteoarthritic cartilage. *Osteoarthritis Cartilage* 22, 1894–1901.
- Bartel, D.P. (2004). MicroRNAs: genomics, biogenesis, mechanism, and function. *Cell* 116, 281–297.
- Lagos-Quintana, M., Rauhut, R., Lendeckel, W., and Tuschl, T. (2001). Identification of novel genes coding for small expressed RNAs. *Science* 294, 853–858.
- Hou, C., Yang, Z., Kang, Y., Zhang, Z., Fu, M., He, A., Zhang, Z., and Liao, W. (2015). MiR-193b regulates early chondrogenesis by inhibiting the TGF- $\beta$ 2 signaling pathway. *FEBS Lett.* 589, 1040–1047.
- Meng, F., Zhang, Z., Chen, W., Huang, G., He, A., Hou, C., Long, Y., Yang, Z., Zhang, Z., and Liao, W. (2016). MicroRNA-320 regulates matrix metalloproteinase-13 expression in chondrogenesis and interleukin-1 $\beta$ -induced chondrocyte responses. *Osteoarthritis Cartilage* 24, 932–941.
- Lee, S., Yoon, D.S., Paik, S., Lee, K.M., Jang, Y., and Lee, J.W. (2014). microRNA-495 inhibits chondrogenic differentiation in human mesenchymal stem cells by targeting Sox9. *Stem Cells Dev.* 23, 1798–1808.
- Kim, Y.J., Kim, H.J., and Im, G.I. (2008). PTHrP promotes chondrogenesis and suppresses hypertrophy from both bone marrow-derived and adipose tissue-derived MSCs. *Biochem. Biophys. Res. Commun.* 373, 104–108.
- Jiang, J., and Hui, C.C. (2008). Hedgehog signaling in development and cancer. *Dev. Cell* 15, 801–812.
- Monroe, D.G., McGee-Lawrence, M.E., Oursler, M.J., and Westendorf, J.J. (2012). Update on Wnt signaling in bone cell biology and bone disease. *Gene* 492, 1–18.
- Gunther, M., Laithier, M., and Brison, O. (2000). A set of proteins interacting with transcription factor Sp1 identified in a two-hybrid screening. *Mol. Cell. Biochem.* 210, 131–142.
- Hsu, C.F., Sui, C.L., Wu, W.C., Wang, J.J., Yang, D.H., Chen, Y.C., Yu, W.C., and Chang, H.S. (2011). Klf10 induces cell apoptosis through modulation of Bcl-1 expression and Ca<sup>2+</sup> homeostasis in estrogen-responding adenocarcinoma cells. *Int. J. Biochem. Cell Biol.* 43, 666–673.
- Jiang, L., Yu, L., Zhang, X., Lei, F., Wang, L., Liu, X., Wu, S., Zhu, J., Wu, G., Cao, L., et al. (2016). miR-892b silencing activates NF- $\kappa$ B and promotes aggressiveness in breast cancer. *Cancer Res.* 76, 1101–1111.
- Cook, T., and Urrutia, R. (2000). TIEG proteins join the Smads as TGF- $\beta$ -regulated transcription factors that control pancreatic cell growth. *Am. J. Physiol. Gastrointest. Liver Physiol.* 278, G513–G521.
- Zhou, S., Eid, K., and Glowacki, J. (2004). Cooperation between TGF- $\beta$  and Wnt pathways during chondrocyte and adipocyte differentiation of human marrow stromal cells. *J. Bone Miner. Res.* 19, 463–470.
- Johnsen, S.A., Subramaniam, M., Janknecht, R., and Spelsberg, T.C. (2002). TGF $\beta$  inducible early gene enhances TGF $\beta$ /Smad-dependent transcriptional responses. *Oncogene* 21, 5783–5790.
- Hawse, J.R., Iwaniec, U.T., Bensamoun, S.F., Monroe, D.G., Peters, K.D., Ilharreborde, B., Rajamannan, N.M., Oursler, M.J., Turner, R.T., Spelsberg, T.C., and Subramaniam, M. (2008). TIEG-null mice display an osteopenic gender-specific phenotype. *Bone* 42, 1025–1031.
- Yan, B., Zhang, Z., Jin, D., Cai, C., Jia, C., Liu, W., Wang, T., Li, S., Zhang, H., Huang, B., et al. (2016). mTORC1 regulates PTHrP to coordinate chondrocyte growth, proliferation and differentiation. *Nat. Commun.* 7, 11151.
- Correa, D., Hesse, E., Seriwatanachai, D., Kiviranta, R., Saito, H., Yamana, K., Neff, L., Atfi, A., Coillard, L., Sitaru, D., et al. (2010). Zfp521 is a target gene and key effector of parathyroid hormone-related peptide signaling in growth plate chondrocytes. *Dev. Cell* 19, 533–546.
- Kozhemyakina, E., Cohen, T., Yao, T.P., and Lassar, A.B. (2009). Parathyroid hormone-related peptide represses chondrocyte hypertrophy through a protein phosphatase 2A/histone deacetylase 4/MEF2 pathway. *Mol. Cell. Biol.* 29, 5751–5762.
- Lisse, T.S., Chun, R.F., Rieger, S., Adams, J.S., and Hewison, M. (2013). Vitamin D activation of functionally distinct regulatory miRNAs in primary human osteoblasts. *J. Bone Miner. Res.* 28, 1478–1488.
- Mraz, M., Dolezalova, D., Plevova, K., Stano Kozubik, K., Mayerova, V., Cerna, K., Musilova, K., Tichy, B., Pavlova, S., Borsky, M., et al. (2012). MicroRNA-650 expression is influenced by immunoglobulin gene rearrangement and affects the biology of chronic lymphocytic leukemia. *Blood* 119, 2110–2113.
- Lee, Y., Kim, M., Han, J., Yeom, K.H., Lee, S., Baek, S.H., and Kim, V.N. (2004). MicroRNA genes are transcribed by RNA polymerase II. *EMBO J.* 23, 4051–4060.
- He, L., and Hannon, G.J. (2004). MicroRNAs: small RNAs with a big role in gene regulation. *Nat. Rev. Genet.* 5, 522–531.
- Mak, K.K., Kronenberg, H.M., Chuang, P.T., Mackem, S., and Yang, Y. (2008). Indian hedgehog signals independently of PTHrP to promote chondrocyte hypertrophy. *Development* 135, 1947–1956.
- Subramaniam, M., Cicek, M., Pitel, K.S., Bruinsma, E.S., Nelson Holte, M.H., Withers, S.G., Rajamannan, N.M., Sretero, F.J., Venuprasad, K., and Hawse, J.R. (2017). TIEG1 modulates  $\beta$ -catenin sub-cellular localization and enhances Wnt signaling in bone. *Nucleic Acids Res.* 45, 5170–5182.
- Chun, J.S., Oh, H., Yang, S., and Park, M. (2008). Wnt signaling in cartilage development and degeneration. *BMB Rep.* 41, 485–494.
- Nalesso, G., Sherwood, J., Bertrand, J., Pap, T., Ramachandran, M., De Bari, C., Pitzalis, C., and Dell’accio, F. (2011). WNT-3A modulates articular chondrocyte phenotype by activating both canonical and noncanonical pathways. *J. Cell Biol.* 193, 551–564.
- Yasuhara, R., Ohta, Y., Yuasa, T., Kondo, N., Hoang, T., Addya, S., Fortina, P., Pacifici, M., Iwamoto, M., and Enomoto-Iwamoto, M. (2011). Roles of  $\beta$ -catenin signaling in phenotypic expression and proliferation of articular cartilage superficial zone cells. *Lab. Invest.* 91, 1739–1752.

36. Golovchenko, S., Hattori, T., Hartmann, C., Gebhardt, M., Gebhard, S., Hess, A., Pausch, F., Schlund, B., and von der Mark, K. (2013). Deletion of beta catenin in hypertrophic growth plate chondrocytes impairs trabecular bone formation. *Bone* 55, 102–112.
37. Geetha-Loganathan, P., Nimmagadda, S., Christ, B., Huang, R., and Scaal, M. (2010). Ectodermal Wnt6 is an early negative regulator of limb chondrogenesis in the chicken embryo. *BMC Dev. Biol.* 10, 32.
38. Cawthorn, W.P., Bree, A.J., Yao, Y., Du, B., Hemati, N., Martinez-Santibañez, G., and MacDougald, O.A. (2012). Wnt6, Wnt10a and Wnt10b inhibit adipogenesis and stimulate osteoblastogenesis through a  $\beta$ -catenin-dependent mechanism. *Bone* 50, 477–489.
39. Dong, Y.F., Soung, Y., Chang, Y., Enomoto-Iwamoto, M., Paris, M., O'Keefe, R.J., Schwarz, E.M., and Drissi, H. (2007). Transforming growth factor- $\beta$  and Wnt signals regulate chondrocyte differentiation through Twist1 in a stage-specific manner. *Mol. Endocrinol.* 21, 2805–2820.
40. Stott, N.S., Jiang, T.X., and Chuong, C.M. (1999). Successive formative stages of precartilaginous mesenchymal condensations in vitro: modulation of cell adhesion by Wnt-7A and BMP-2. *J. Cell. Physiol.* 180, 314–324.
41. Guo, X., Day, T.F., Jiang, X., Garrett-Beal, L., Topol, L., and Yang, Y. (2004). Wnt/ $\beta$ -catenin signaling is sufficient and necessary for synovial joint formation. *Genes Dev.* 18, 2404–2417.
42. Kato, M., Patel, M.S., Levasseur, R., Lobov, I., Chang, B.H., Glass, D.A., 2nd, Hartmann, C., Li, L., Hwang, T.H., Brayton, C.F., et al. (2002). Cbfa1-independent decrease in osteoblast proliferation, osteopenia, and persistent embryonic eye vascularization in mice deficient in Lrp5, a Wnt coreceptor. *J. Cell Biol.* 157, 303–314.
43. Subramaniam, M., Harris, S.A., Oursler, M.J., Rasmussen, K., Riggs, B.L., and Spelsberg, T.C. (1995). Identification of a novel TGF- $\beta$ -regulated gene encoding a putative zinc finger protein in human osteoblasts. *Nucleic Acids Res.* 23, 4907–4912.
44. Fautsch, M.P., Vrabel, A., Rickard, D., Subramaniam, M., Spelsberg, T.C., and Wieben, E.D. (1998). Characterization of the mouse TGF $\beta$ -inducible early gene (TIEG): conservation of exon and transcriptional regulatory sequences with evidence of additional transcripts. *Mamm. Genome* 9, 838–842.
45. Yoshida, C.A., Yamamoto, H., Fujita, T., Furuichi, T., Ito, K., Inoue, K., Yamana, K., Zanma, A., Takada, K., Ito, Y., and Komori, T. (2004). Runx2 and Runx3 are essential for chondrocyte maturation, and Runx2 regulates limb growth through induction of Indian hedgehog. *Genes Dev.* 18, 952–963.
46. Hawse, J.R., Cicek, M., Grygo, S.B., Bruinsma, E.S., Rajamannan, N.M., van Wijnen, A.J., Lian, J.B., Stein, G.S., Oursler, M.J., Subramaniam, M., and Spelsberg, T.C. (2011). TIEG1/KLF10 modulates Runx2 expression and activity in osteoblasts. *PLoS ONE* 6, e19429.
47. Lee, J.M., and Im, G.I. (2012). PTHrP isoforms have differing effect on chondrogenic differentiation and hypertrophy of mesenchymal stem cells. *Biochem. Biophys. Res. Commun.* 421, 819–824.